Eur. J. Biochem. **270**, 745–756 (2003) © FEBS 2003 doi:10.1046/j.1432-1033.2003.03436.x

Unusual fluorescence of W168 in *Plasmodium falciparum* triosephosphate isomerase, probed by single-tryptophan mutants

Priyaranjan Pattanaik[1], Gudihal Ravindra[2], Chandana Sengupta[2], Kapil Maithal[2], Padmanabhan Balaram[2] and Hemalatha Balaram[1]

[1]*Molecular Biology and Genetics Unit, Jawaharlal Nehru Centre for Advanced Scientific Research, Bangalore, India;* [2]*Molecular Biophysics Unit, Indian Institute of Science, Bangalore, India*

Plasmodium falciparum triosephosphate isomerase (PfTIM) contains two tryptophan residues, W11 and W168. One is positioned in the interior of the protein, and the other is located on the active-site loop 6. Two single-tryptophan mutants, W11F and W168F, were constructed to evaluate the contributions of each chromophore to the fluorescence of the wild-type (wt) protein and to probe the utility of the residues as spectroscopic reporters. A comparative analysis of the fluorescence spectra of PfTIMwt and the two mutant proteins revealed that W168 possesses an unusual, blue-shifted emission (321 nm) and exhibits significant red-edge excitation shift of fluorescence. In contrast, W11 emits at 332 nm, displays no excitation dependence of fluorescence, and behaves like a normal buried chromophore. W168 has a much shorter mean lifetime (2.7 ns) than W11 (4.6 ns). The anomalous fluorescence properties of W168 are abolished on unfolding of the protein in guanidinium chloride (GdmCl) or at low pH. Analysis of the tryptophan environment using a 1.1-Å crystal structure established that W168 is rigidly held by a complex network of polar interactions including a strong hydrogen bond from Y164 to the indole NH group. The environment is almost completely polar, suggesting that electrostatic effects determine the unusually low emission wavelength of W168. To our knowledge this is a unique observation of a blue-shifted emission from a tryptophan in a polar environment in the protein. The wild-type and mutant proteins show similar levels of enzymatic activity and secondary and tertiary structure. However, the W11F mutation appreciably destabilizes the protein to unfolding by urea and GdmCl. The fluorescence of W168 is shown to be extremely sensitive to binding of the inhibitor, 2-phosphoglycolic acid.

Keywords: fluorescence lifetime; *Plasmodium falciparum*; red-edge excitation shift; single tryptophan mutant; triosephosphate isomerase.

Triosephosphate isomerase (TIM) is an important glycolytic enzyme that catalyses the isomerization of dihydroxyacetone phosphate and glyceraldehyde 3-phosphate. Like most TIMs, the enzyme from the malarial parasite *Plasmodium falciparum* (PfTIM) is a homodimer of $(\alpha/\beta)_8$ barrels. Each monomer has a central core of β-strands surrounded by α-helices [1]. Such a fold is commonly known as the TIM fold [2] and 10–12% of all known enzyme structures fall into this category [3–5]. This fold is also predicted to be the most abundant in the proteome of an organism [6,7]. The diversity of function and evolutionary significance has made the $(\alpha/\beta)_8$ barrel a major target for structural studies [8–10].

PfTIM is being used in our laboratory as a model system for studying folding and assembly of dimeric proteins. Studies on folding of PfTIM and site-directed interface mutants [11,12], along with related studies reported in the literature [13,14], suggest that formation of folded monomers precedes association into functional dimers, in the folding pathway of TIM. While PfTIM unfolds in guanidinium chloride (GdmCl) solution, it maintains a considerable level of secondary, tertiary and quaternary structure in 8 M urea [11]. A detailed elucidation of the structural events during unfolding is facilitated if spectroscopic probes are located at key points in the protein structure. PfTIM contains two tryptophan residues, at positions 11 and 168 (Fig. 1). Alignment of sequences of 89 known TIMs has revealed that W168 is completely conserved, whereas other aromatic residues may replace W11. W168 is present on loop 6, which undergoes significant dynamic changes, with residues 166–176 moving as a rigid body, both in the presence and absence of ligand [15–17]. Loop 6 is also referred to as the catalytic loop, as it closes over the active site when substrate binds. W11 is part of the N-terminal segment of the dimer interface, although the indole ring itself is directed towards the interior of the monomeric unit. Analysis of the fluorescence properties of PfTIM under diverse conditions is complicated by overlap of contributions of individual tryptophan residues. To dissect the specific contributions of each chromophore to the spectral properties of the protein, we constructed two mutants, W11F and W168F, each of which contains a single

Correspondence to H. Balaram, Molecular Biology and Genetics Unit, Jawaharlal Nehru Centre for Advanced Scientific research, Jakkur, Bangalore, India 560 064.
Fax: + 91 80 8462766, Tel.: + 91 80 8462750 ext. 2239,
E-mail: hb@jncasr.ac.in

Abbreviations: TIM, triosephosphate isomerase; PfTIM, triosephosphate isomerase from *Plasmodium falciparum*; GdmCl, guanidinium chloride; REES, red-edge excitation shift.

(Received 8 August 2002, revised 4 December 2002, accepted 17 December 2002)

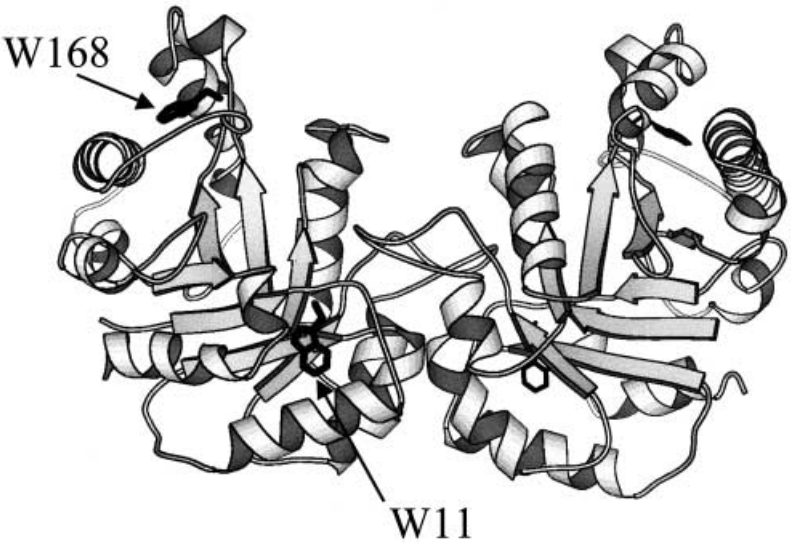

Fig. 1. Crystal structure of PfTIM [44] dimer. Both tryptophans in one monomer are labelled. The diagram was generated using MOLSCRIPT [54].

tryptophan residue. Several recent studies have established the utility of single-tryptophan mutants in the interpretation of protein emission spectra [18–24]. Theoretical analysis has also emphasized the importance of single-tryptophan proteins in understanding the role of the microenvironment in determining the emission properties of the indole chromophore [25,26].

Normally, low-wavelength (< 330 nm) emissions have been associated with hydrophobic environments around tryptophan residues in proteins, and only red-shifted fluorescence is taken to indicate polar environments. In this report, we establish that W168 in PfTIM exhibits unusual fluorescence properties, an extremely low wavelength of emission, low quantum yield, and short lifetime. These features are rationalized on the basis of a network of polar interactions revealed by a high-resolution crystal structure. Also, W168 fluorescence is shown to be sensitive to inhibitor binding. Replacing tryptophan with phenylalanine at the two sites leads to changes in the stability of the mutant proteins in the presence of denaturants, as revealed by spectroscopic studies, with the W11F mutant being significantly destabilized.

Materials and methods

Reagents

α-Glycerol phosphate dehydrogenase, NADH and glyceraldehyde-3-phosphate dehydrogenase were purchased from Sigma Chemical Co., St Louis, MO, USA and used without further purification. The substrate glyceraldehyde-3-phosphate was obtained as a diethylacetal monobarium salt and processed to its active form according to the manufacturer's instructions. The concentration of glyceraldehyde 3-phosphate extracted was estimated using glyceraldehyde-3-phosphate dehydrogenase. Restriction enzymes and T4 DNA ligase were obtained from Amersham Pharmacia, UK. *Taq* DNA polymerase was from Bangalore Genei Private Limited, Bangalore, India. All other chemicals were obtained locally and were of the highest grade. Conditions recommended by the manufacturer were used for all molecular biology reagents. The *Escherichia coli* strain AA200 was a gift from Dr Barbara Bachmann of the *E. coli* Genetic Stock Center New Haven, CT, USA.

Mutagenesis, protein expression and purification

The plasmid pTIM-C1 [27] carrying PfTIM in the expression vector pTrc99A was used to construct the single tryptophan mutants. The oligonucleotide 5′-CACCATGG CTAGAAAATATTTTGTCGCAGCAAAC**TTC**AAAT GTAA-3′, in which the codon for Trp (TGG) was mutated to that for Phe (TTC), along with a 3′-gene-specific primer (5′-ACGGATCCTTACATAGCACTTTTTATTATATC-3′) was used to amplify the mutant TIM gene (W11F) using pTIMC1 as template. The PCR conditions used were as follows: for a volume of 50 μL, 10 ng pTIMC1, 200 ng of each primer, 2.5 mM dNTP mixture, and 5 U *Taq* polymerase were used. The buffer supplied by the enzyme manufacturer was used for the PCR. The PCR cycle conditions were denaturation at 93 °C for 15 s followed by annealing at 50 °C for 20 s and extension at 73 °C for 15 s. Thirty cycles of PCR yielded enough product for further utilization. The amplified fragment was gel purified, digested with restriction enzymes *Nco*I and *Bam*HI, and ligated with the appropriately cut vector, pTrc99A. The ligation mix was used to transform the *E. coli* strain AA200 (*garB*10, *fhuA*22, *ompF*627, *fadL*701, *relA*1, *pit*-10, *phoM*510, *merB*1), which lacks endogenous TIM activity. One of the recombinants selected was verified to carry the required mutation by partial DNA sequencing. The complete sequence of W11F was further confirmed by electrospray MS analysis of the purified enzyme and of the fragments obtained by tryptic digestion. W168F was constructed using the method of mega-primer PCR [28]. The mutagenic primer (5′-TTA**TTC**GCTATTGG TACTGGTA-3′) along with the above mentioned 3′ primer was used to amplify the mega-primer using pTIMC1 as template. The conditions used for PCR were same as above. This 3′ TIM fragment of 260 bp was gel purified and used as

mega-primer along with the 5′-gene-specific primer, 5′-CAG AATTCCATGGCTAGAAAATATTTTGTCGC-3′ for the second PCR. The reaction mixture contained the same concentration of the various components as described above except for the mega-primer, which was kept at 400 ng. Thirty cycles of denaturation at 93 °C for 45 s followed by annealing at 68 °C for 30 s and extension at 73 °C for 30 s were carried out. Cloning of this mutant TIM fragment into pTrc99A and subsequent transformation into AA200 was performed in a manner similar to that described for W11F. One of the clones selected was verified for the presence of the required sequence by electrospray MS analysis on the purified recombinant protein. Here again, both the full-length protein and proteolytic fragments obtained after trypsin treatment were analysed.

Expression and purification of the mutants were carried out using methodology reported previously [11] for wild-type PfTIM. Briefly, AA200 cells transformed with the recombinant plasmid were induced using 5 $g \cdot L^{-1}$ lactose at an A_{600} of 0.8. The culture broth was further supplemented with same amount of lactose twice at intervals of 4 h. TIM was purified from bacterial lysates by precipitation with ammonium sulfate at a saturation of 70–90% followed by anion-exchange chromatography using a ResourceQ (6 mL; Pharmacia) column at pH 8.0 (20 mM Tris/HCl) with a linear gradient of 0–0.5 M NaCl. Finally, gel filtration using Sephacryl S200 (HR16/60 column; Pharmacia) was carried out to obtain homogeneous TIM. Protein was stored at −20 °C as a lyophilized powder until use. All protein determinations were carried out using the Bradford method [29] with BSA as standard.

Enzyme assay

Kinetic measurements were carried out by the method of Plaut and Knowles [30] in a Shimadzu UV210A double-beam spectrophotometer at room temperature. The cuvette contained 100 mM triethanolamine buffer, pH 7.6, 5 mM EDTA, 0.5 mM NADH, α-glycerophosphate dehydrogenase (20 $\mu g \cdot mL^{-1}$) and 0.16–2.4 mM glyceraldehyde 3-phosphate. Enzyme activity was determined by monitoring the decrease in A_{340}. The dependence of the initial rate on the substrate concentration was analysed according to the Michaelis–Menten equation. The values for the kinetic parameters (K_m and k_{cat}) were calculated from Lineweaver–Burk plots.

Fluorescence measurements

Fluorescence emission spectra were recorded on an Hitachi 650–60 or Perkin–Elmer LS-55 spectrofluorimeter. The protein samples were excited at 270 nm or 295 nm and the emission spectra recorded from 300 nm to 400 nm. Excitation and emission band-pass was kept as 5 nm.

Time domain fluorescence lifetime measurements were carried out using the single-photon counting method. A continuous wave diode pump laser with a doubling crystal that generated light at a wavelength of 1064 nm was used to pump a Ti-sapphire laser (Tsunami, Spectra Physics, CA, USA). The source of excitation (295 nm) was the third harmonic of the fundamental Ti-sapphire wavelength. This setup was able to produce light at a repetition rate of 4 MHz with a pulse width of less than 2 ps. The detector was a MCP-PMT (Hamamatsu Photonics, Japan). Decay curves were acquired in 500–600 channels of 50 ps/channel to about 10 000 counts in the peak. Data were analysed using the software provided by the manufacturers. The analysis of decay assumed a multiexponential model:

$$I(t) = \sum_i \alpha_i \exp(-t/\tau_i)$$

with amplitudes α_i and lifetimes τ_i. Goodness of fit was derived from χ^2_R values and the weighted residuals. The relative contribution of each decay component f_i to the total emission was calculated as:

$$f_i = \frac{\alpha_i \tau_i}{\sum_j \alpha_j \tau_j}$$

Circular dichroism

CD measurements were carried out on a JASCO J-715 spectropolarimeter. Ellipticity changes at 220 nm and 280 nm were monitored to follow the unfolding transition. A path length of 1 mm was used in the far-UV and a 5-mm-path length cuvette was used for the near-UV CD. Spectra were averaged over four scans at a scan speed of 10 $nm \cdot min^{-1}$.

Mass spectrometry

Electrospray ionization mass spectra were recorded on a Hewlett-Packard (model HP-1100) electrospray mass spectrometer coupled to an online 1100 series HPLC. Electrospray ionization was carried out using a capillary with an internal diameter of 0.1 mm. The tip was held at 5000 V in a positive ion detection mode. Nebulization was assisted by N_2 gas (99.8%) at a flow rate of 10 $L \cdot min^{-1}$. The spray chamber was held at 300 °C. The ion optics zone was optimized for maximal ion transmission. The best signal was obtained when a declustering potential (fragmentor voltage) of 200 V was set for detection. Data were acquired across a suitable mass range using a conventional quadrupole with cycle time of 3 s. The spectrometer was tuned using five calibration standards provided by the manufacturer. Data were processed using the deconvolution module of the CHEMSTATION software to detect multiple charge states and obtain derived masses.

Size-exclusion chromatography

Analytical gel filtration was carried out using a calibrated Superdex 75H gel-filtration column (10 mm internal diameter × 300 mm) fitted to an Akta Basic HPLC from Amersham-Pharmacia, Uppsala, Sweden. The protein sample was eluted at a flow rate of 0.5 $mL \cdot min^{-1}$ with 20 mM Tris/HCl, pH 8.0, containing 150 mM NaCl. The effect of urea on the quaternary structure of the protein was monitored by incubating at the desired concentration of denaturant for 30 min before passing the sample through the gel-filtration column equilibrated at the same urea concentration.

Monitoring of inhibitor binding to PfTIM and the mutants

Quenching of Trp fluorescence in all three proteins after binding of TIM inhibitor 2-phosphoglycolic acid was monitored at emission maxima of each protein following excitation at 295 nm. Protein concentration in each case was maintained at 1 μM. Aliquots of 0.5 μL of a 20-mM stock solution of 2-phosphoglycolic acid were added to 0.5 mL TIM at pH 8.0 (20 mM Tris/HCl). Emission intensities were monitored after incubation for 20 min at room temperature. Measurements were carried out until there was no further decrease in fluorescence intensity. 2-Phosphoglycolic acid at the highest concentration had no effect on the absorbance of the protein solution at 295 nm.

Results and discussion

Expression, purification and characterization of mutants

Wild-type TIM (TIMwt) and both the mutants (W11F and W168F) were expressed in the *E. coli* strain AA200 (null for TIM). All the proteins were purified to homogeneity from the cell lysates and their constitution confirmed by SDS/PAGE followed by electrospray MS of both intact and tryptic digests of purified proteins (data not shown). Masses of 27832 and 27792 Da were observed for the wild-type and mutant proteins, respectively, under conditions of electrospray where only the protein monomers are detected. The calculated masses for wild-type and mutants are 27831.5 and 27792.5, respectively. Further, the masses of the tryptic peptides generated by digests of the mutant proteins confirmed the positions of the mutations to be as desired (data not shown).

Purified TIM and the mutants were checked for enzymatic activity using a coupled enzyme assay. Table 1 summarizes the kinetic parameters of enzyme activities of the three proteins. Although the Michaelis–Menten constants (K_m) for the mutants were comparable to the wild-type, the k_{cat} values were almost twofold lower than that of the wild-type enzyme, probably because of the mutations being close to active-site residues (in the case of W11F) or in segments involved in catalysis (in the case of W168F). The W168F mutant of yeast TIM has been reported to have a similar decrease of ≈40% in the catalytic efficiency [31].

The extinction coefficients at 280 nm were determined to be 31 400 $M^{-1}\cdot cm^{-1}$ for TIMwt and 25 710 $M^{-1}\cdot cm^{-1}$ for the two tryptophan mutants. Normalized UV-absorption spectra for the two mutants showed that the overall shapes of the spectra were quite similar to that of the wild-type protein, with absorption maxima at 278 nm (data not shown).

Table 1. Kinetic parameters for TIMwt and mutants. G3P, Glyceraldehyde 3-phosphate.

Protein	K_m for G3P (mM)	k_{cat} (min^{-1})
TIMwt	0.36–0.43	2.68×10^5
W11F	0.25–0.41	1.55×10^5
W168F	0.30–0.36	1.57×10^5

The far-UV CD spectra of the mutant and the wild-type proteins revealed that the overall secondary structures of all three proteins are quite similar (Fig. 2A). The near-UV CD spectra, which measure the asymmetric environment of the aromatic residues in the protein, showed a slight decrease in the ellipticity of both the mutants compared with that of TIMwt (Fig. 2B). The aromatic CD of PfTIM is dominated by the contributions from the tyrosine residues, and the small decrease in ellipticity is probably the result of replacement of one tryptophan by phenylalanine, rather than loss of tertiary structure as a consequence of the mutations. The absence of significant variation in kinetic parameters and CD spectra supports the existence of similar overall 3D structures in the mutant and wild-type TIMs,

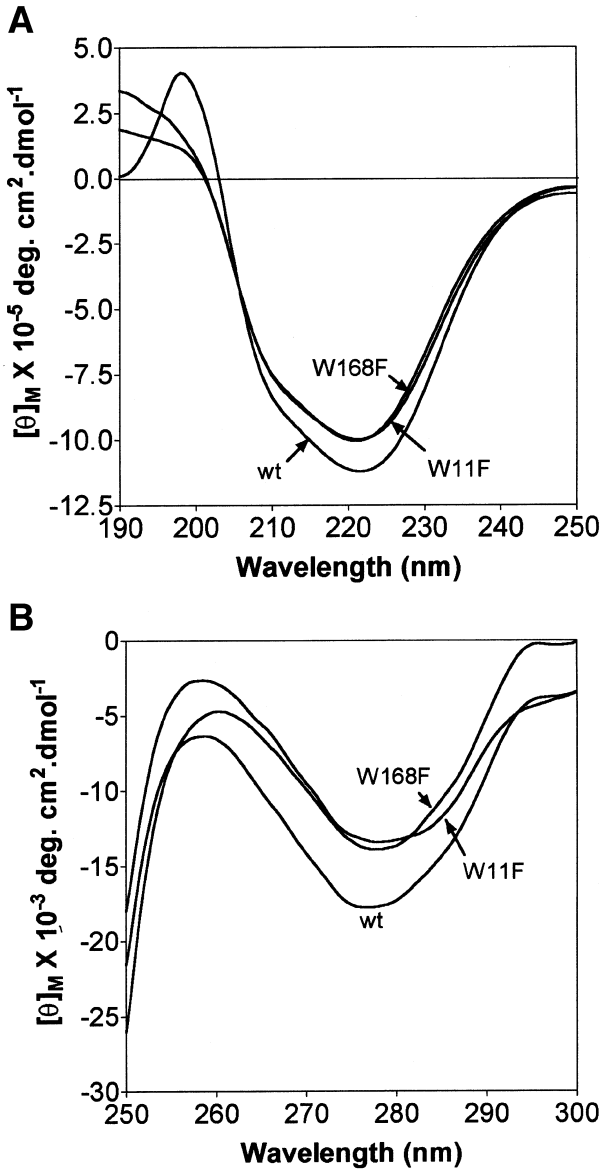

Fig. 2. CD spectra of PfTIM wild-type (wt) and mutants (W11F, W168F). (A) Far UV; (B) near UV. Protein concentrations were 4.0 and 32.0 μM for far-UV and near-UV CD measurements, respectively.

justifying the use of these single tryptophan mutants for detailed fluorescence analysis.

Fluorescence properties

Steady-state fluorescence emission was recorded after excitation at 270 nm (Fig. 3A) or 295 nm (Fig. 3B). In the case of excitation at 270 nm, no distinct peak corresponding to emission from tyrosine residues (at 308 nm) was observed. TIMwt and mutant W168F had emission maxima at 331 and 332 nm, respectively, whereas mutant W11F emitted at 321 nm. Emission spectra were recorded after excitation at 295 nm (Fig. 3B) in order to minimize the contribution of tyrosine residues to total emission. The emission maxima for TIMwt and W168F were almost unchanged, but interestingly, the emission maximum for W11F was at 327 nm, red-shifted by about 6 nm. Compared with TIMwt, there was a substantial fall of 70% in the fluorescence intensity of W11F, while W168F showed a decrease of about 30%. This suggests that the contribution of W168 to overall protein fluorescence is quite low. To study the effect of excitation wavelength on emission maxima, all three proteins were subjected to excitation at different wavelengths over the range 280–305 nm, and emission maxima at each wavelength of excitation were monitored. As shown in Fig. 3 (inset), there was very little dependence of emission wavelength on excitation wavelength in the case of TIMwt and W168F, but W11F shows a progressive red shift of 7 nm with increasing excitation wavelength from 290 nm to 305 nm. A difference in emission maxima after excitation at the red edge of the absorption spectrum is commonly known as red-edge excitation shift (REES), a feature observed in many proteins [32–34]. This phenomenon is generally attributed to the restricted motion of the tryptophan residue. REES is also indicative of a heterogeneous environment due to variation in locations of polar groups in the vicinity of the tryptophan [35].

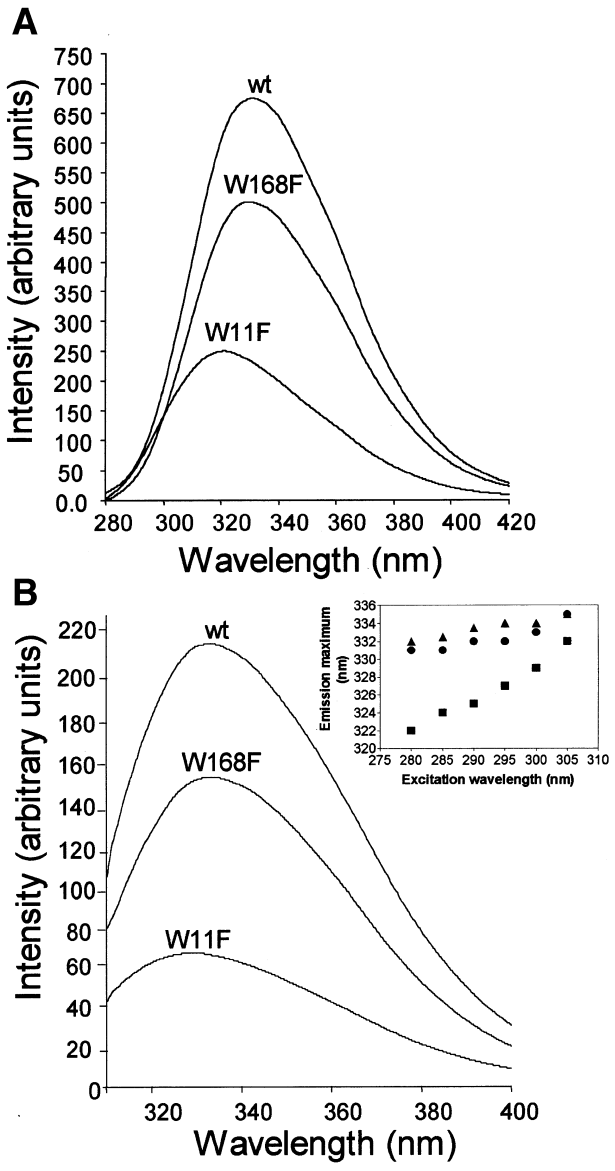

Fig. 3. Steady-state fluorescence emission spectra of PfTIM wild-type (wt) and single tryptophan mutants (W11F and W168F) at pH 8.0. Spectra were recorded after excitation at 270 nm (A) or 295 nm (B). Inset, Dependence of fluorescence emission maxima of TIMwt (●), W11F (■) and W168F (▲) on excitation wavelength. Protein concentrations were kept at 0.5 μM.

Fluorescence decay curves were recorded for the wild-type and mutant TIMs at pH 8.0 in order to estimate excited state lifetimes. Emission wavelengths were set at the respective emission maxima of each protein under the given condition. At pH 8.0, tryptophan fluorescence decays were described adequately by two-exponential models for all three proteins. The χ^2_R values, characterizing the goodness of fit, were always less than 1.2, and the weighted residuals were randomly distributed around zero. Attempted fits of the experimental data to a single exponential model showed very large increases in χ^2_R values. A three-exponential fit led to no improvement in χ^2_R values or generated the third term with very short lifetimes in the subnanosecond range. The parameters associated with the time-resolved fluorescence in TIMwt and its single-tryptophan mutants are summarized in Table 2. In all three cases the major decay component was characterized by a longer lifetime (3–4.9 ns), while the other component had a significantly shorter decay time (1.5–1.8 ns). Notably, the value of the major decay component for W168 in mutant W11F was appreciably shorter (3.0 ns).

The comparative analysis of the properties of the three proteins PfTIMwt, W11F and W168F suggests that the emission properties of W168 are unusual. This residue displays a significantly blue-shifted emission (321 nm), with the emission wavelength showing significant REES. In addition, fluorescence of W168 is appreciably quenched and it also yields a significantly lower lifetime than W11. In contrast, W11 yields an emission maximum of 332 nm in the folded protein characteristic of a buried Trp and shows no evidence of excitation wavelength dependence of emission. Furthermore, W11 has a significantly higher quantum yield of emission than that of W168. Figure 4 shows the immediate environments of the two Trp residues in PfTIM, as observed in the crystal structure of an enzyme–inhibitor complex determined at 1.1 Å resolution. Remarkably, W168 is located in an environment that contains several

Table 2. Fluorescence lifetimes for PfTIM and mutants.

Protein	Condition	Emission wavelength (nm)[a]	χ^2	τ_1 (ns)	τ_2	τ_3	f_1 (%)	f_2	f_3	Mean lifetime $\langle\tau\rangle$
Wild-type	pH 8.0	332	0.98	–	1.8	4.6	–	27.6	72.4	3.8
	pH 2.8	346	1.10	0.2	1.5	4.6	4.5	32.3	63.2	3.4
	6 M GdmCl	357	1.15	0.1	1.19	3.7	5.3	31.5	63.2	2.7
W11F	pH 8.0	327	1.12	–	1.5	3.0	–	26.0	74.0	2.7
	pH 2.8	340	1.05	0.2	1.4	4.4	3.7	30.8	65.5	3.3
	6 M GdmCl	357	1.10	0.1	1.0	3.5	4.4	25.6	70.0	2.8
W168F	pH 8.0	334	1.10	–	1.5	4.9	–	7.5	92.5	4.6
	pH 2.8	340	1.05	0.3	1.4	4.5	5.6	34.0	60.4	3.2
	6 M GdmCl	357	1.07	0.2	1.0	2.8	6.9	38.5	54.6	1.9

[a] Lifetime measurements for each protein under specified conditions were carried out at these wavelengths of emission.

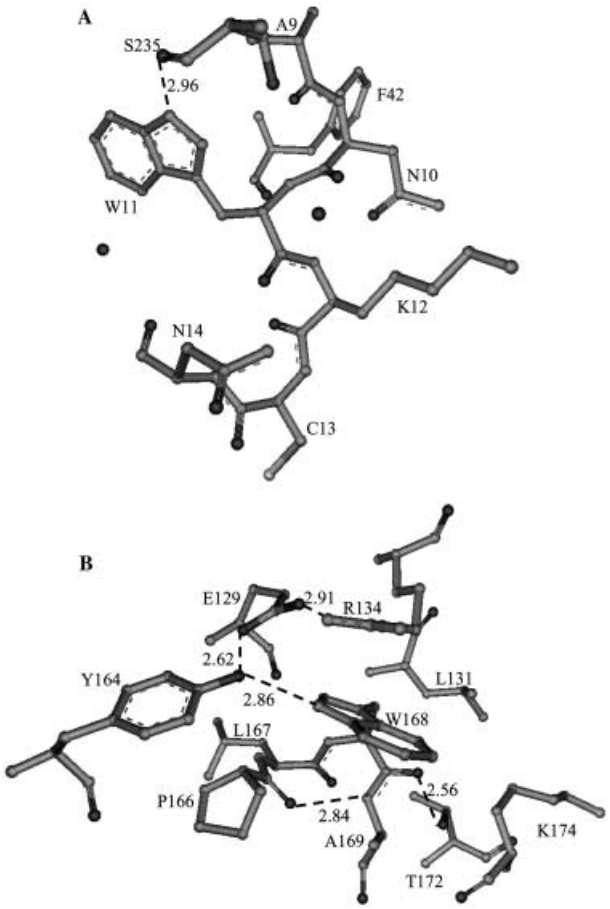

Fig. 4. Amino-acid environments around W11 (A) and W168 (B). Residues that are at a minimum distance of 3.5 Å from the tryptophans are shown. The figures were generated from a 1.1-Å crystal structure [44] of PfTIM using a Swiss-pdb viewer [55]. Hydrogen bonds are shown as dotted lines along with the distances in Å.

polar residues, including E129 and R134. Indeed the plane of the guanidino group of R134 is roughly parallel to the indole ring of W168 with a short distance of approach of 3.24 Å between the indole and one of the N atoms of the guanidino group. Importantly, the phenolic O atom of Y164 forms a good hydrogen bond with the indole NH of W168 (N–0 2.86 Å). A strong network of local hydrogen bonds stabilizes the cluster of residues in the vicinity of W168. The carboxylate of E129 forms H-bonds to both the phenolic hydroxyl of Y164 (O–O 2.62 Å) and the guanidino group of R134 (O–N 2.91 Å). Further, L167 and W168 occupy the $i + 1$ and $i + 2$ positions of a type 1 β-turn stabilized by a backbone hydrogen bond between P166 CO and A169 NH (N—O 2.84 Å). Another short hydrogen bond between W168 CO and T172 OH (O–O 2.56 Å) completes the network of polar interactions, which immobilizes the W168 residue. Indeed the indole ring of W168 makes no close nonpolar contact. Inspection of the crystal structure thus reveals a highly polar, but frozen environment for W168. Hence, any local movements about the available degrees of freedom, backbone or side chain would be expected to have very high activation barriers, as several networked interactions would have to be disrupted. Clearly, the unusual emission properties of W168 are a consequence of its local electrostatic environment and its immobility. The importance of electrostatic effects in modulating Trp fluorescence shifts in proteins has recently been stressed, invoking the concept of an internal Stark effect [25]. The quenching of W168 fluorescence may be a consequence of the several interactions detailed above [25,36]. Notably, involvement of the indole NH group in hydrogen-bonding has also been shown to quench Trp emission in proteins [37]. Indeed, the only other proteins that exhibit emission maxima further shifted to shorter wavelengths are azurin (308 nm), calpactin (314 nm), parvalbumin (316 nm) and *E. coli* asparginase (319 nm) [38]. Examination of the structures of azurin and parvalbumin indicates that the blue-shifted emission arises from the single tryptophan residue located in the highly hydrophobic environment. In the case of azurin, mutagenesis of the two hydrophobic residues I7 and F110 to serine (located in the vicinity of W48) leads to a red shift of the emission maximum [39,40]. Apart from this study, W59 in RNase T_1 is probably the only other example (to our knowledge) of a tryptophan, localized in an environment containing polar residues and ordered water molecules, emitting at a low-emission wavelength of 322 nm [25,41].

W11 is in a moderately nonpolar environment with the indole NH involved in a hydrogen bond with the S235 backbone CO group (O—N 2.96 Å). Solvent accessibility calculations [42] reveal that both W11 and W168 are relatively inaccessible to water molecules (relative accessibilities calculated for tryptophan side chains in A subunit were 0.5% for W11 and 6.9% for W168). It may be noted that the dimer interface segments of PfTIM are composed of interacting loops, with W11 lying away from the subunit interface.

Comparison of fluorescence properties of folded and denatured proteins

In a fully folded protein, spectral properties of the indole chromophore are largely dictated by the surrounding environment, resulting in observable differences for specific tryptophan residues. However, under conditions of complete denaturation, such differences are minimized and similar fluorescence properties may be expected, irrespective of the position of the chromophore in the structure of the protein. The addition of 6 M GdmCl completely abolishes tertiary structure in TIM. Steady-state emission spectra in the presence of 6 M GdmCl (Fig. 5A) showed a large red shift (357 nm) in the emission maxima characteristic of tryptophan in a completely solvent-exposed environment. As expected, there was no difference in the emission maxima of all three proteins. There was a significant fall in the fluorescence intensities under these conditions. Significantly, the relative contributions of each tryptophan towards the overall emission of the wild-type protein changed compared with that at pH 8.0. The emission intensity of W11F was $\approx$60% of that of the wild-type, and that of W168F was $\approx$40%. In 6 M GdmCl there was no excitation dependence of the emission from W11F. As noted above, this mutant exhibited a prominent REES at pH 8.0. The excited state lifetime values for all proteins under unfolding conditions are listed in Table 2. Under these conditions, better fits to experimental data were obtained using a three-exponential model, although the amplitudes of the third components were relatively small. The decay times characterizing the major components are very similar for TIMwt and W11F mutant (3.66 and 3.54 ns). Curiously, the lifetime of the W168F mutant was appreciably shorter (2.8 ns). The possibility of local structural effects that influence lifetimes in the unfolded state cannot be ruled out in this case.

Previous studies have established that TIMwt exists as an expanded molten globule at pH 2.8 which retains significant secondary structure but lacks tertiary interactions, as evidenced by CD and binding to the hydrophobic dye ANS [43]. Fluorescence measurements were also carried out for all three proteins at pH 2.8 (Fig. 5B). The emission maxima after excitation at 295 nm were 348 nm for TIMwt and W168F and 346 nm for W11F. Significant red shifts in all three proteins indicated structural changes resulting in exposure of the tryptophan side chains. As in the case of completely denatured proteins, the contribution of Trp168 to the overall fluorescence of TIMwt was higher (65% of TIMwt) than that of Trp11 (40% of TIMwt). Time-resolved decay curves for all the proteins at pH 2.8 were satisfactorily fitted to a three-exponential model with the slowest decaying components having the largest amplitudes

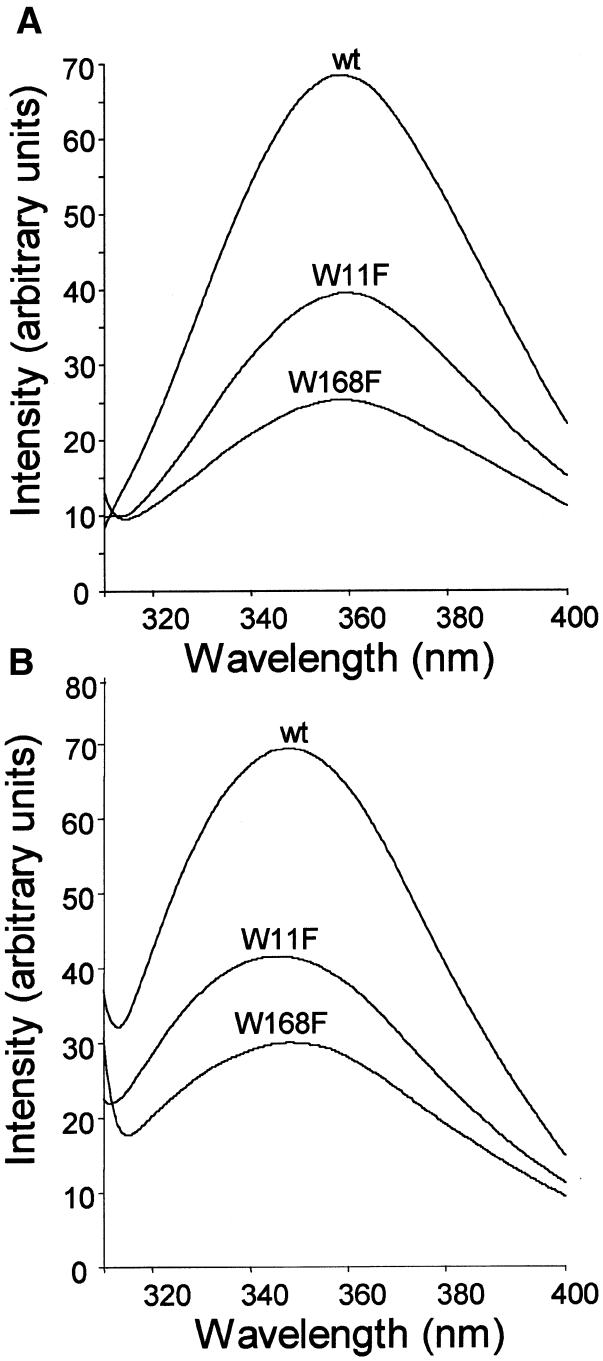

Fig. 5. Steady-state emission spectra of PfTIM wild type (wt) and single-tryptophan mutants (W11F and W168F) in the presence of 6 M GdmCl (A) and at pH 2.8 (B). Protein concentrations of 0.5 μM were maintained in each case.

(Table 2). Lifetime components for all three proteins showed no significant differences under these conditions.

Stability of the mutants

In engineering single-tryptophan mutants in PfTIM, we have made the assumption that the Trp to Phe replacement will not cause significant structural alterations. This expectation

has been borne out by the almost unimpaired enzymatic activity of the mutant proteins. However, inspection of the high-resolution (1.1 Å) crystal structure of the native protein [44] suggested that significant disruption of local interactions may result as a consequence of mutation, with a concomitant reduction in overall stability of the protein under denaturing conditions. We therefore carried out spectroscopic studies on all three proteins in both urea and GdmCl to evaluate their relative stabilities under unfolding conditions. PfTIM has been previously shown to possess considerable structure even in 8 M urea but has been shown to unfold in GdmCl. Unfolding was monitored by fluorescence in terms of shift in emission maxima and fall in intensity (Fig. 6). In the case of TIMwt, up to a concentration of 6 M urea, there was no significant change in the emission maximum (λ_{em}) and the emission intensity fell by only 30–40%. However, there was a sharp change in the emission intensity between 6 and 8 M urea, suggesting a significant change in the tryptophan environment. The C_m values (concentration of urea at which 50% of the protein is unfolded) for W11F and W168F were

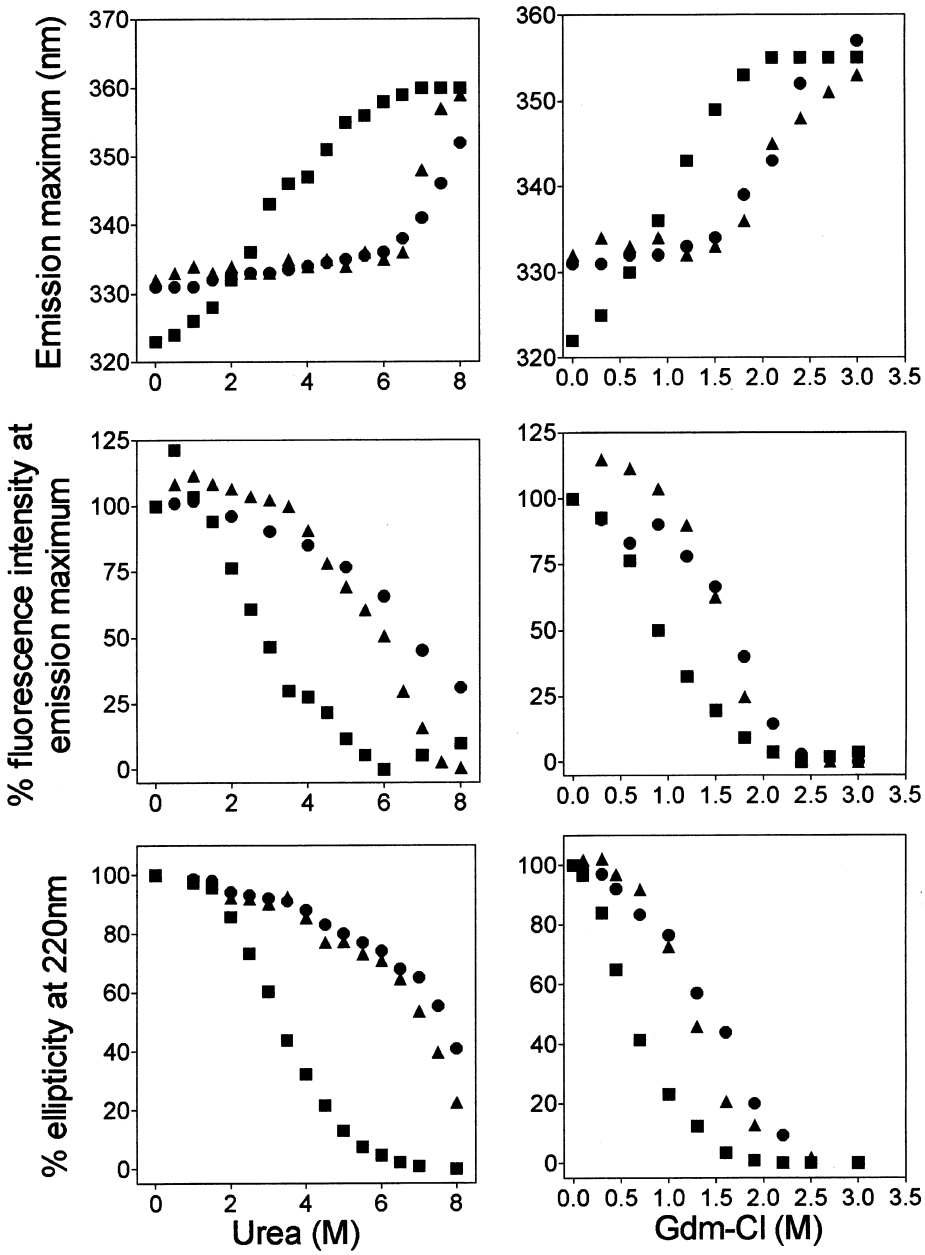

Fig. 6. Equilibrium unfolding of PfTIM wild-type (●), W11F (■) and W168F (▲) using urea (left column) and GdmCl (right column) as denaturants. Extent of denaturation was monitored by measuring the fall in emission intensity (middle row) at 331, 332 and 227 nm for PfTIMwt, W168F and W11F, respectively. Fluorescence intensities in the absence of denaturant were taken as 100%. Unfolding was also monitored by a change in emission maxima (top row) with increasing concentrations of the denaturant and by a fall in ellipticity at 220 nm (bottom row). The excitation wavelength for the fluorescence measurements was kept at 295 nm. A protein concentration of 4.0 μM was used in each case.

3.0 M and 6.0 M, respectively (Fig. 6), suggesting that the W11F is significantly more susceptible to denaturation by urea than W168F, which behaves similar to the wild-type enzyme. Similar observations were made when GdmCl was used as a denaturant, where TIMwt, W11F and W168F had C_m values of 1.2, 0.5 and 1.1 M, respectively (Fig. 6). The changes in the secondary structure of the two proteins with urea were also monitored using far-UV CD measurements at 220 nm. As shown in Fig. 6, TIMwt and W168F retained substantial secondary structure in concentrations of urea as high as 6 M, whereas, the secondary structure of W11F collapsed completely in 5 M urea. These results suggest that the W11F mutation significantly enhances the susceptibility of the protein to unfolding induced by urea and GdmCl. Inspection of the crystal structure reveals that W168, which is positioned on loop 6, has a local environment largely determined by the loop residues, which are proximal in sequence (Fig. 4B). Replacement of this residue with Phe may be expected to have little effect on the overall stability of the protein, and indeed this expectation is borne out by the experimental data. In contrast, W11 is located in the interior of the protein and makes several apolar contacts with the proximal residues (Fig. 4A). Replacement by a much smaller residue, Phe, would be expected to generate a cavity, which would then require structural readjustment of neighbouring residues to optimize packing. In general, cavity-creating mutations lead to destabilization of protein structure [45–49]. Indeed, W11F shows significantly greater susceptibility to unfolding induced by urea and GdmCl than TIMwt and W168F. Destabilization of the native state in the W12F mutant of *Trypanosoma brucei* TIM has been shown recently [50].

Urea-induced denaturation of TIMwt and the mutants was also monitored as a function of increase in their Stoke's radii using gel filtration as a tool. As shown in Fig. 7, the retention volumes of the mutant proteins were exactly the same as that of TIMwt under native conditions. In the case of the wild-type enzyme, even at 8 M urea the dimer did not dissociate completely into monomers. In contrast, the entire population was eluted as solvated monomers in the case of both the mutants at concentrations much below 8 M. In addition, W11F showed an aggregated intermediate at 3 M urea, which disappeared when the concentration of the denaturant was increased. Such an aggregate was entirely lacking in the course of unfolding of W168F. Aggregation may be brought about by exposure of hydrophobic patches on the surface of the partially unfolded protein.

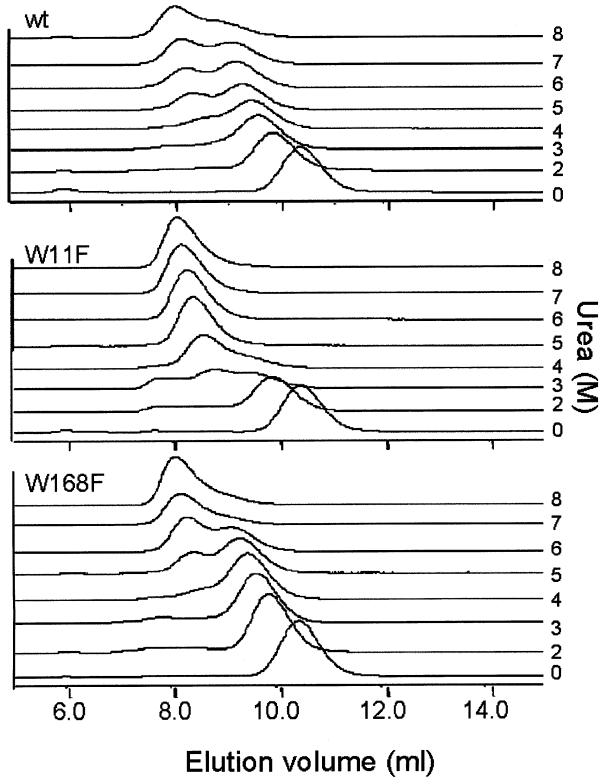

Fig. 7. Denaturaration of PfTIM (top), W11F (middle) and W168F (bottom) as monitored by gel filtration in the presence of urea (see Materials and methods for details). Concentrations of urea used are indicated on the right of each chromatogram.

Probing inhibitor binding with Trp fluorescence

Inhibitor binding to TIM has been shown to result in a major movement of loop 6 (residues 166–176), which contains the W168 residue. Although crystal structures of enzyme–inhibitor complexes have largely yielded the loop-closed conformation in the bound form, in the case of PfTIM several complexes of inhibitors and substrate analogs have been shown to adopt the loop-open conformation [44]. The complex of the transition-state analog 3-phosphoglycolate has been shown to adopt both open and closed conformations of the loop in crystals [44]. The proximity of W168 to the substrate-binding site suggests that this residue may prove to be a useful spectroscopic probe for monitoring ligand–protein interactions. Figure 8 shows the effect of the inhibitor 2-phosphoglycolic acid on Trp emission. In the case of TIMwt, there is very little change in intensity over a wide range of inhibitor concentrations. As discussed above, the emission spectrum of TIMwt is largely dominated by contributions from W11, with W168 being considerably quenched with an unusually blue-shifted emission maximum. The availability of the single-tryptophan mutants W11F and W168F provides an opportunity to examine whether ligand binding does indeed influence the properties of the tryptophan residue in loop 6. The effects of inhibitor on the fluorescence intensity of the two mutant proteins are shown in Fig. 8. Interestingly, there is a dramatic reduction in the fluorescence intensity of W11F upon inhibitor binding, suggesting that complex formation has an appreciable effect on the chromophoric properties of W168. In the case of W168F, there is a small, but nevertheless significant increase in fluorescence intensity on inhibitor binding. W11 is present next to the active-site residue K12, which is involved in positioning the substrate or inhibitor. It is conceivable that the enhancement of W11 fluorescence on complex formation may be the consequence of local structural changes in the vicinity of the active site.

Conclusions

Fluorescence spectroscopy provides a convenient and sensitive means of probing the environment of tryptophan

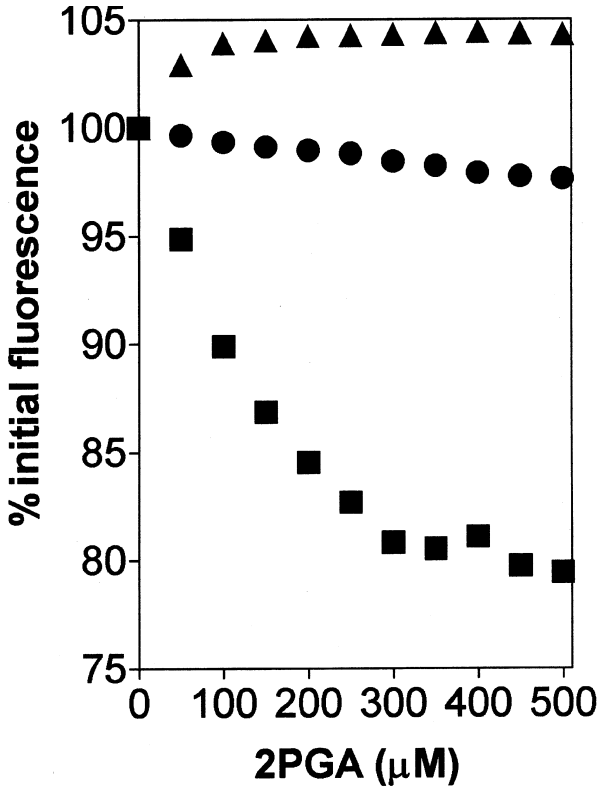

Fig. 8. Effect of inhibitor binding on fluorescence emission. PfTIM wild-type (●), mutants W11F (■) and W168F (▲) were incubated in the presence of increasing concentrations of inhibitor 2-phosphoglycolic acid. Fluorescence intensities were recorded at the maxima after excitation at 295 nm and plotted as percentage of the intensities in the absence of inhibitor. A protein concentration of 1 μM in 20 mM Tris/HCl, pH 8.0, was used in each case.

residues in proteins [51,52]. The utility of intrinsic protein fluorescence is limited by the fact that many proteins contain multiple tryptophan residues making interpretation of resultant spectra ambiguous. Site-directed mutagenesis provides a powerful means of replacing tryptophan residues, generating single-tryptophan mutants. PfTIM contains two tryptophan residues at positions 11 and 168 providing an opportunity to probe distinctly different segments of the protein structure and to interpret protein fluorescence on the basis of available structural data. To enable unambiguous spectral interpretation, we examined the single-tryptophan mutants W11F and W168F. The results establish that the properties of W168 are extremely unusual, with a blue-shifted emission at 321 nm and a very low quantum yield of fluorescence emission compared with that of W11 and the wild-type. In addition, W168 also exhibits a significant excitation dependence of its emission. The high-resolution crystal structure of PfTIM provides a rationalization of the unusual spectroscopic properties of W168, which is frozen in an extremely polar environment. The anomalous wavelength of emission is presumably dictated by the electrostatic environment of the chromophore, consistent with recent theoretical calculations [25,26]. W11 exhibits the spectroscopic properties characteristic of an indole chromophore buried in the hydrophobic interior of a protein. Although transfer of indole chromophores from polar solvents to nonpolar solvents results in a blue shift in the fluorescence maximum, it must be stressed that structural interpretations of unusually blue-shifted chromophores must be made with caution. As noted in the case of W168, a tryptophan residue surrounded largely by polar groups can exhibit an extremely low wavelength of emission. It is also important to stress that, at present, interpretation of fluorescence parameters, such as emission wavelengths, quantum yields and excited state lifetimes, cannot be made in terms of local structural features in the vicinity of the chromophore. Overviews of existing data do not reveal any readily apparent correlation between emission wavelengths and fluorescence lifetimes or between emission wavelengths and quantum yields, for Trp residues in proteins [53]. However, the availability of single-tryptophan mutants in a structurally well-characterized system suggests that future analysis of mutational effects on protein fluorescence may provide useful additional insights. The utility of single-tryptophan mutants has been confirmed by establishing that the fluorescence of the W11F mutant is sensitive to inhibitor binding, in contrast with the wild-type protein.

Acknowledgements

Time resolved fluorescence measurements were carried out at the National Centre for Ultra-fast Processes at the University of Madras, Chennai, supported by the Department of Science and Technology, Govt of India. The help of Professor P. Ramamurthy and Dr I. Priyadarshini in measuring fluorescence decay is gratefully acknowledged. We thank Professor M. R. N. Murthy and Dr S. Parthasarathy, Molecular Biophysics Unit, Indian Institute of Science for providing the co-ordinates of the PfTIM crystal structure at 1.1 Å. H.B. acknowledges financial assistance from the Department of Science and Technology and, Council of Scientific and Industrial Research, India.

References

1. Velanker, S.S., Ray, S.S., Gokhale, R.S., Suma, S., Balaram, H., Balaram, P. & Murthy, M.R.N. (1997) Triosephosphate isomerase from *Plasmodium falciparum*: the crystal structure provides insights into antimalarial drug design. *Structure* **5**, 751–761.
2. Wierenga, R.K. (2001) The TIM-barrel fold: a versatile framework for efficient enzymes. *FEBS Lett.* **492**, 193–198.
3. Farber, G.K. & Petsko, G.A. (1990) The evolution of alpha/beta barrel enzymes. *Trends Biochem. Sci.* **6**, 228–234.
4. Reardon, D. & Farber, G.K. (1996) The structure and evolution of alpha/beta barrel proteins. *FASEB J.* **10**, 184.
5. Pujadas, G. & Palau, J. (1999) TIM barrel fold: structural, functional and evolutionary characteristics in natural and designed molecules. *Biologia Bratislava* **53**, 231–254.
6. Gerstein, M. (1997) A structural census of genomes: comparing bacterial, eukaryotic, and archaeal genomes in terms of protein structure. *J. Mol. Biol.* **274**, 562–576.
7. Hegyi, H. & Gerstein, M. (1999) The relationship between protein structure and function: a comprehensive survey with application to the yeast genome. *J. Mol. Biol.* **288**, 147–164.
8. Mainfroid, V., Terpstra, P., Beauregard, M., Frere, J.M., Mande, S.C., Hol, W.G., Martial, J.A. & Goraj, K. (1996) Three human TIM mutants that provide new insights on why TIM is a dimer. *J. Mol. Biol.* **257**, 441–456.

9. Kursula, I., Partanen, S., Lambeir, A.M., Antonov, D.M., Augustyns, K. & Wierenga, R.K. (2001) Structural determinants for ligand binding and catalysis of triosephosphate isomerase. *Eur. J. Biochem.* **268**, 5189–5196.
10. Borchert, T.V., Abagyan, R., Jaenicke, R. & Wierenga, R.K. (1994) Design, creation, and characterization of a stable, monomeric triosephosphate isomerase. *Proc. Natl. Acad. Sci. USA* **91**, 1515–1518.
11. Gokhale, R.S., Ray, S.S., Balaram, H. & Balaram, P. (1999) Unfolding of *Plasmodium falciparum* triosephosphate isomerase in urea and guanidinium chloride: evidence for a novel disulfide exchange reaction in a covalently cross-linked mutant. *Biochemistry* **38**, 423–431.
12. Gopal, B., Ray, S.S., Gokhale, R.S., Balaram, H., Murthy, M.R.N. & Balaram, P. (1999) Cavity-creating mutation at the dimer interface of *Plasmodium falciparum* triosephosphate isomerase: restoration of stability by disulfide cross-linking of subunits. *Biochemistry* **38**, 478–486.
13. Zabori, S., Rudolf, R. & Jaenicke, R. (1980) Folding and association of triose phosphate isomerase from rabbit muscle. *Z. Naturforsch.* **35**, 999–1004.
14. Waley, S.G. (1973) Refolding of triose phosphate isomerase. *Biochem. J.* **135**, 165–172.
15. Pompliano, D.L., Peyman, A. & Knowles, J.R. (1990) Stabilization of a reaction intermediate as a catalytic device: definition of the functional role of the flexible loop in triosephosphate isomerase. *Biochemistry* **29**, 3186–3194.
16. Rozovsky, S., Jogl, G., Tong, L. & McDermott, A.E. (2001) Solution-state NMR investigations of triosephosphate isomerase active site loop motion: ligand release in relation to active site loop dynamics. *J. Mol. Biol.* **310**, 271–280.
17. Rozovsky, S. & McDermott, A.E. (2001) The time scale of the catalytic loop motion in triosephosphate isomerase. *J. Mol. Biol.* **310**, 259–270.
18. Demchenko, A.P., Gryczynski, I., Gryczynski, Z., Wiczk, W., Malak, H. & Fishman, M. (1993) Intramolecular dynamics in the environment of the single tryptophan residue in staphylococcal nuclease. *Biophys. Chem.* **48**, 39–48.
19. Tcherkasskaya, O., Bychkova, V.E., Uversky, V.N. & Gronenborn, A.M. (2000) Multisite fluorescence in proteins with multiple tryptophan residues. Apomyoglobin natural variants and site-directed mutants. *J. Biol. Chem.* **275**, 36285–36294.
20. Shen, W.H. (1993) Fluorescence lifetimes of the tryptophan residues in ornithine transcarbamoylase. *Biochemistry* **32**, 13925–13932.
21. Nath, U. & Udgaonkar, J.B. (1997) Folding of tryptophan mutants of barstar: evidence for an initial hydrophobic collapse on the folding pathway. *Biochemistry* **36**, 8602–8610.
22. Martensson, L., Jonasson, P., Freskgard, P., Svensson, M., Carlsson, V. & Jonsson, B. (1995) Contribution of individual tryptophan residues to the fluorescence spectrum of native and denatured forms of human carbonic anhydrase II. *Biochemistry* **34**, 1101–1121.
23. Soulages, J.L. & Arrese, E.L. (2000) Fluorescence spectroscopy of single tryptophan mutants of apolipophorin-III in discoidal lipoproteins of dimyristoylphosphatidylcholine. *Biochemistry* **39**, 10674–10580.
24. Engelborghs, Y. & Fersht, A. (2000) Barnase: fluorescence analysis of a three tryptophan protein. In *Topics in Fluorescence Spectroscopy* (Lakowicz, J. R., ed.), Vol. 6, pp. 83–102. Kluwer Academic, New York, USA.
25. Vivian, J.T. & Callis, P.R. (2001) Mechanisms of tryptophan fluorescence shifts in proteins. *Biophys. J.* **80**, 2093–2109.
26. Callis. P.R. (1997) 1La and 1Lb transitions of tryptophan: applications of theory and experimental observations to fluorescence of proteins. *Methods Enzymol.* **278**, 113–150.
27. Ranie, J., Kumar, V.P. & Balaram, H. (1993) Cloning of the triosephosphate isomerase gene of *Plasmodium falciparum* and expression in *Escherichia coli*. *Mol. Biochem. Parasitol.* **61**, 159–170.
28. Sarkar, G. & Sommer, S.S. (1995) The megaprimer method of site directed mutagenesis. *Biotechniques*. **8**, 404–407.
29. Bradford, M.M. (1976) A rapid and sensitive method for the quantitation of microgram quantities of protein utilizing the principle of protein-dye binding. *Anal. Biochem.* **72**, 248–254.
30. Plaut, B. & Knowles, J.R. (1972) pH-dependence of the triose phosphate isomerase reaction. *Biochem. J.* **129**, 311–320.
31. Sampson, N.S. & Knowles, J.R. (1992) Segmental movement: definition of the structural requirements for loop closure in catalysis by triosephosphate isomerase. *Biochemistry* **31**, 8482–8487.
32. Demchenko, A.P. (1988) Red-edge-excitation fluorescence spectroscopy of single-tryptophan proteins. *Eur. Biophys. J.* **16**, 121–129.
33. Demchenko, A.P. & Ladokhin, A.S. (1988) Red-edge-excitation fluorescence spectroscopy of indole and tryptophan. *Eur. Biophys. J.* **15**, 369–379.
34. Demchenko, A.P. (1986) *Ultraviolet Spectroscopy of Proteins*. Springer-Verlag, Berlin, Germany.
35. Mukherjee, S. & Chattopadhyay, A. (1995) Wavelength-selective fluorescence as a novel tool to study organization and dynamics in complex biological systems. *J. Fluorescence* **5**, 237–246.
36. Chen, Y. & Barkley, M.D. (1998) Toward understanding tryptophan fluorescence in proteins. *Biochemistry* **37**, 9976–9982.
37. Nanda, V. & Brand, L. (2000) Aromatic interactions in homeodomains contribute to the low quantum yield of a conserved, buried tryptophan. *Proteins* **40**, 112–125.
38. Eftink, M.R. (1991) Fluorescence techniques for studying protein structure. *Methods Biochem. Anal.* **35**, 127–205.
39. Gilardi, G., Mei, G., Rosato, N., Canters, G.W. & Finazzi-Agro, A. (1994) Unique environment of Trp48 in *Pseudomonas aeruginosa* azurin as probed by site-directed mutagenesis and dynamic fluorescence spectroscopy. *Biochemistry* **33**, 1425–1432.
40. Hammann, C., Messerschmidt, A., Huber, R., Nar, H., Gilardi, G. & Canters, G.W. (1996) X-ray crystal structure of the two site-specific mutants Ile7Ser and Phe110Ser of azurin from *Pseudomonas aeruginosa*. *J. Mol. Biol.* **255**, 362–366.
41. Axelsen, P.H. & Prendergast, F.G. (1989) Molecular dynamics of tryptophan in ribonuclease-T1. II. Correlations with fluorescence. *Biophys. J.* **56**, 43–66.
42. Hubbard, S.J. & Thornton, J.M. (1993) '*Naccess*', *Computer Program*. Department of Biochemistry and Molecular Biology, University College, London, UK.
43. Ray, S.S., Singh, S.K. & Balaram, P. (2001) An electrospray ionisation mass spectrometry investigation of 1-anilino-8-naphthalene-sulfonate (ANS) binding to proteins. *J. Am. Soc. Mass. Spetrom.* **4**, 428–438.
44. Parthasarathy, S. (2001) Structural studies on *Plasmodium Falciparum* triosephosphate isomerase and analysis of atomic displacement parameters in high resolution protein structures. PhD Thesis, Indian Institute of Science, Bangalore, India.
45. Baldwin, E.P. & Matthews, B.W. (1994) Core-packing constraints, hydrophobicity and protein design. *Curr. Opin. Biotechnol.* **5**, 396–402.
46. Varadarajan, R. & Richards, F.M. (1992) Crystallographic structures of ribonuclease S variants with nonpolar substitution at position 13: packing and cavities. *Biochemistry* **31**, 12315–12327.
47. Jackson, S.E., Moracci, M., el Masry, N., Johnson, C.M. & Fersht, A.R. (1993) Effect of cavity-creating mutations in the

hydrophobic core of chymotrypsin inhibitor 2. *Biochemistry* **32**, 11259–11269.
48. Stites, W.E., Gittis, A.G., Lattman, E.E. & Shortle, D. (1991) In a staphylococcal nuclease mutant the side-chain of a lysine replacing valine 66 is fully buried in the hydrophobic core. *J. Mol. Biol.* **221**, 7–14.
49. Hubbard, S.J. & Argos, P. (1995) Evidence on close packing and cavities in proteins. *Curr. Opin. Biotechnol.* **6**, 375–381.
50. Chanez-Cardenas, M.E., Fernandez-Velasco, D.A., Vazquez-Contreras, A., Coria, R., Saab-Rincon, G. & Perez-Montfort, R. (2002) Unfolding of triosephosphate isomerase from *Trypanosoma brucei*: identification of intermediates and insight into the denaturation pathway using tryptophan mutants. *Arch. Biochem. Biophys.* **399**, 117–129.
51. Demchenko, A.P. (1991) Fluorescence and dynamics in proteins. In *Topics in Fluorescence Spectroscopy* (Lakowicz, J.R., ed.), Vol. 3, pp. 65–112. Plenum press, New York, USA.
52. Lakowicz, J.R. (2000) On spectral relaxation in proteins. *Photochem. Photobiol.* **72**, 421–437.
53. Eftink, M.R. (2000) Intrinsic fluorescence of proteins. In *Topics in Fluorescence Spectroscopy* (Lakowicz, J.R., ed.), Vol. 6, pp. 1–16. Kluwer Academic, New York, USA.
54. Kraulis, P.J. (1991) MOLSCRIPT: a program to produce both detailed and schematic plots of protein structures. *J. Appl. Crystallogr.* **24**, 946–953.
55. Guex, N. & Peitsch, M.C. (1997) SWISS-MODEL and the Swiss-PdbViewer: an environment for comparative protein modelling. *Electrophoresis* **18**, 2714–2723.